

# TRANSFER LEARNING MODEL FOR BRAIN TUMOR DETECTION WITH SNAKE SEGMENTATION

Manisha Tyagi and Priyanka

Department of Electronics and Communication Engineering, Deenbandhu Chhotu Ram University of Science and Technology, India

## Abstract

*As medical standards advance, the role of medical imaging in clinical diagnosis and monitoring becomes increasingly vital. This paper presents a novel approach for the detection and classification of brain tumors using MRI imaging, leveraging digital image processing and artificial intelligence with a focus on Transfer Learning. The methodology begins with pre-processing MRI scans using a Gaussian filter, followed by snake segmentation for image partitioning. The images are then de-noised using a Parallel Non-Local Mean filter. For classification, a hybrid model combining a pre-trained VGG16 network with a Convolutional Neural Network is proposed, capitalizing on the advantages of transfer learning. This model's efficacy is benchmarked against conventional machine learning algorithms—SVM, KNN, RF—and other deep learning architectures, including CNN variations with AlexNet, self-attention, and additive attention. Implemented in Python on Google Colab, the model was trained and tested on a Kaggle dataset comprising 5,712 images. Metrics employed for evaluation included accuracy, precision, and recall, alongside execution time. The findings demonstrate that our proposed transfer learning-enhanced model achieved superior performance with an accuracy of 96.7%, precision of 96%, and recall of 95%, thus outstripping the other examined models in brain tumor detection efficiency.*

## Keywords:

Brain Tumor, Snake Segmentation, PNLM Filter, VGG16, CNN

## 1. INTRODUCTION

Brain tumors, which consist of abnormal cell growths within the brain, pose significant challenges to neurological function and overall health. With their varied presentations and increasing incidence, brain tumors have emerged as a critical area of research in medicine [1]. Diagnosis typically relies on the careful evaluation of imaging data, often through magnetic resonance imaging. However, such analyses are subject to variability based on the interpreting physician's expertise, potential visual fatigue, and the breadth of their medical knowledge. This underscores the crucial need for precise and consistent methods to detect brain tumors from imaging studies

Malignant brain tumors are characterized by uncontrollable proliferation of brain tissues, with the potential to significantly raise intracranial pressure, hence injuring healthy brain tissue and potentially leading to death [2]. These cancerous growths, particularly gliomas—which account for approximately 40% of central nervous system malignancies—tend to be aggressive and are often associated with low survival rates. Nonetheless, timely and accurate detection of such tumors can be pivotal in developing effective treatment strategies, thereby improving patient outcomes. The intricacy of brain architecture combined with the often subtle manifestations that can be mistaken for less severe conditions, like migraines, renders the identification of advanced-stage gliomas from MR images an endeavour [3].

The automated diagnosis of brain tumors has seen considerable advancement in recent years, fostered by a surge in innovative approaches reported in the literature. These strides are largely attributable to technological progress in machine learning and image processing. Magnetic resonance imaging is a non-invasive modality that eschews harmful ionizing radiation, providing detailed insights into tissue and organ structure with high-resolution imagery. MRI not only refines the diagnostic process by potentially reducing the need for invasive exploratory surgeries such as thoracotomies or laparotomies and offers reliability for lesion localization and preoperative planning [4].

Brain tumor diagnosis using MRI involves advanced imaging techniques, such as 3D multi-band imaging, which offers benefits over traditional 2D imaging by providing precise coordinates for accurate lesion localization. This allows clinicians to determine the exact positioning of the tumor [5]. MRI's capability to acquire multiple images of the same tissue region enhances the diagnostic process. Image pre-processing is a crucial step that significantly impacts the performance of image segmentation, recognition, and detection systems. To improve the performance of deep learning algorithms, various image pre-processing methods, including image enhancement and skull-stripping, are utilized. Skull stripping is particularly important as it removes non-brain structures, including the skull, from MRI scans, thus facilitating more focused analysis [6]. Due to the adverse effects of low contrast in original images on classifier performance, image augmentation techniques are often employed. Additionally, noise reduction filters are applied prior to augmentation to minimize artifacts from image acquisition and transmission, ultimately enhancing image quality for better feature extraction [7].

Accurate segmentation of brain tumors from neuroimaging data is essential for planning and monitoring clinical trials, as well as enhancing the detection of these diseases. Given the variability in location, size, and shape of brain tumors, precise segmentation is a complex task that involves determining not only the tumor's boundaries but also its exact position and dimensions [8]. Automatic image processing tools, such as region-based segmentation, take into account factors like region homogeneity, spatial proximity, and pixel characteristics when merging pixels to achieve distinct delineation of tumor regions [9].

Feature extraction plays a pivotal role in the research methodology, where it involves distilling an element's inherent attributes and representing them as distinct characteristics of an image. The primary objective of this phase is to extract various features based on intensity [10]. Among the prevalent texture metrics utilized is the Gray-Level Co-occurrence Matrix texture. This technique serves as a fundamental method for quantifying the frequency at which pairs of pixels with specific intensity values  $i$  and  $j$  occur in a predetermined spatial relationship. This relationship is defined by the distance and angle between the pixel pair. Subsequently, the intensity-based features, also known as

gray levels, of the input images are ascertained through the analysis of histograms [11].

Moving on to the categorization or classification stage, which is deemed the most crucial in the proposed research work, it involves identifying the category to which the image belongs [12]. Several common classification algorithms are utilized for locating brain tumors, including Support Vector Machines (SVM), neural networks (NNs), Random Forest (RF), and others. SVM, known for its proficiency in generalization, aims to discover the hyperplane with the largest margin among the training samples [13]. It stands as a renowned machine learning method grounded in statistical learning theory, seeking to linearly partition the data by projecting it onto a higher-dimensional feature space. The advantage of the SVM method lies in its efficient generalization of a classification problem.

Neural Networks (NNs) are statistical learning methods inspired by the functioning of the human brain. A network of fundamental artificial neurons interconnected with each other forms the basis of NNs [14]. These connections are established using adaptive weights that are adjusted over time. Although NNs were extensively employed for classification tasks, their usage gradually diminished due to the computational demands, leading to a preference for simpler methods like SVM.

The advent of deep learning techniques, particularly Convolutional Neural Networks (CNN), gained popularity due to their success in international image and speech recognition challenges. CNNs have demonstrated excellent results in classifying medical imaging and tumor diagnosis problems.

## 2. RELATED WORKS

Abdel-Gawad, et al. [15] introduced an optimized technique based on a genetic algorithm. A mechanism was presented as an application for detecting the boundary line of the tumor from a human brain MRI scan image. Primary BCET helped to improve the image features for offering superior attributes of medical images. Subsequently, GA was utilized to detect the fine edges on a suitable training dataset. The analysis revealed the supremacy of the introduced method over the traditional techniques. The accuracy of the introduced method was calculated at 99.09%, and FOM was 85.59%.

Kumar et al. [16] presented a lightweight DL method and an effective compression method with the aim to improve the quality of an image and its accuracy. The images were classified accurately when the error was diminished. WOA was integrated with the BWO algorithm to diagnose the tumor. The grading of the tumor was detected with the help of this hybrid method. MRI scans were used to analyze the outcomes of the presented method concerning DC, accuracy and sensitivity. The results showed that the presented method yielded superior performance when compared with the earlier techniques.

Thachayani et al. [17] designed a hybrid of CNN and SSAE algorithms to diagnose the tumor in brain MRI. This hybrid approach led to enhance the accuracy and efficacy of classification of the tumor. The proposed approach was simulated using MATLAB software on a dataset of 120 scans. The acquired findings verified that the designed approach could be applied to the classification and grading of brain Tumors using magnetic resonance imaging images.

Islam, et al. [18] suggested a TK model based on an improved technique with superpixels and PCA for diagnosing tumors in the brain in the least execution time [18]. To extract meaningful features, PCA and superpixels are first used. After that, a filter was used to improve the image in order to increase accuracy. In the end, the TK-Means algorithm's image segmentation helped with the Tumor diagnosis procedure. This led to the identification of the brain Tumor. The testing results showed that, in comparison to earlier systems, the suggested method for identifying brain Tumors in MRI images improved accuracy and shortened execution times.

Derea, et al. [19] projected a software for detecting and recognizing brain tumors. RoI (region of interest) was detected in MRI (Magnetic Resonance Imaging) scans through a SBT (segmentation-based threshold) model. To extract texture properties, the grey-level run length matrix approach (GRLM) was used. After that, MRI images were examined for Tumors using the SBT approach. For each feature in the MRI, the histogram and behaviour complement images helped identify the Tumor. The geometric parameters of size, position, area, and dimensions were used to evaluate both the Tumor image and the complement image. It was discovered that the outcomes were ideal for dividing the entire Tumor area. After isolating the complement area from the Tumor zone, the GRLM algorithm yielded a greater accuracy.

[20] designed a FCSE-GAN for segmenting the brain tumor region in Magnetic Resonance Imaging. The neural network model that was used was called ResNet. In order to produce the sharp MRI (Magnetic Resonance Imaging) scans and segment the brain Tumor region using a discriminator, the approach of concatenating the attributes was utilised. The experimentation's planned strategy was assessed using the Kaggle dataset. The experimental findings showed that the planned strategy fared extremely well in terms of a number of parameters.

Srinivasa Reddy et al. (2021) discussed that this study concentrated on investigating the tumor regions in MRI scans with the implementation of DL and optimization techniques [21]. RGB images were converted to grayscale before image processing to boost the intensity of the resulting grayscale image. The skull stripping method was utilised to remove the skull, tissue, and splints. The segmented images were classified using the CNN method. The results of the studies showed that the accuracy, sensitivity, and specificity were maximised using the CNN-MSO (CNN-Modified Spider Optimisation) algorithm.

Jian et al. [22] introduced a method which relied on saliency modelling to diagnose the brain tumor on MRI scans. Initially, a morphological plan to remove Magnetic Resonance Imaging images from the skull helped to lessen its impact. Second, a saliency-detection method based on principal local contrast (PLC) was used to enhance the foreground regions that made it possible to identify the lesion region. Finally, the image was de-noised, and morphological and segmentation operations were performed to improve the results. Following experimentation, the MRI data demonstrated the reliability and efficacy of the newly presented technique.

Shah et al. [23] established a DCNN recognized as an EfficientNet-B0 algorithm with layers to classify and detect the brain tumor effectively. A variety of filters were used to improve the scan quality. The methods for enhancing the data samples

were implemented. The results showed that, when compared to the current approaches, the proposed model provided better accuracy and AUC values, indicating greater accuracy. When categorising the Tumor, the algorithm’s accuracy was found to be 98.87.

Kabir et al. [24] described that detecting and diagnosing the brain tumor at the initial phase led to alleviating the death rate. An algorithm for detecting the tumor was put forward, which relied on SVM and ANN. This algorithm had diverse stages such as preserving the gradient intensity smoothing-based edge, enhancing the image and segmenting it, extracting the attributes and classifying the image. BRATS dataset was used in the presented algorithm. The experimental outcome depicted that the presented algorithm yielded an accuracy of 97.7% in contrast to other method.

In contrast to these related studies, ours uses unique approach by applying snake segmentation in segmentation phase followed by applying PNLM filters and using transfer learning approach for the classification stage for the process of detection and classification of brain tumors in human MRI images. In essence, transfer learning in deep learning represents a paradigm shift by allowing models to leverage knowledge acquired from one task to improve performance on another. This approach addresses some of the challenges associated with training deep networks from scratch and has led to more practical and resource-efficient applications of deep learning in various domains.

### 3. MATERIAL AND METHODS

#### 3.1 SPECIFICATIONS OF IMAGE DATA SET

In this study, we evaluate the efficacy of our proposed methodology using the Kaggle dataset, which comprises MR images with dimensions of 512\*512 pixels. The dataset encompasses a total of 5712 images, each paired with corresponding labels. Our proposed approach is designed to categorize brain MRI scans into four groups: Glioma, Meningioma, Pituitary, and no tumor. The implementation of our model is carried out on Google Colab, leveraging Tensorflow and Keras in the Python programming language. Google Colab provides a computing environment with 12 GB of RAM, 50GB of hard drive space, and free GPU access.

The selected dataset includes images featuring brain tumors such as Glioma, Meningioma, and pituitary, alongside images of healthy brains. The distribution of the dataset among the different classes is presented in Table.1. Notably, the dataset also incorporates healthy brain MRI images, appropriately labeled as “no-tumor.” The dataset is composed of four classes, as illustrated in Fig.1, with a distribution that is relatively balanced, ranging from 25 to 30 percent across the classes. There is no overfitting concern during prediction, and the classes exhibit a fair balance. The dataset is divided into two subsets – training data and testing data – approximately in an 80:20 ratio. The Brain MR dataset comprises 4284 training images with corresponding labels. In exploring the application of snake segmentation for Region of Interest (ROI) extraction and tumor prediction using our proposed approach, a test dataset consisting of 1428 distinct magnetic resonance images was employed. A selection of sample images from the dataset is showcased in Fig.2.

Table.1. Dataset Distribution

| No. of MRI images in dataset |              |                         |
|------------------------------|--------------|-------------------------|
| Brain images                 | Class Labels | No. of images available |
| Normal                       | No Tumor     | 1595                    |
| Abnormal                     | Glioma       | 1321                    |
|                              | Meningioma   | 1339                    |
|                              | Pituitary    | 1457                    |
| <b>Total</b>                 |              | <b>5712</b>             |

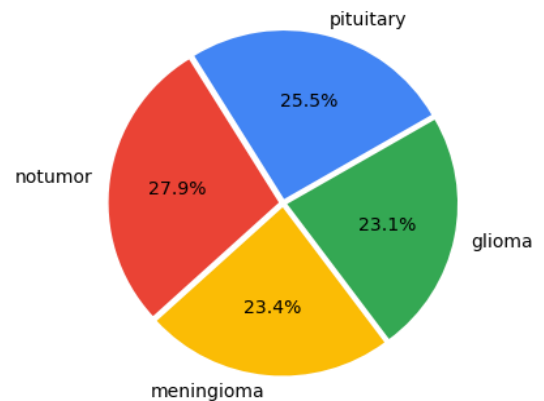


Fig.1. Dataset Class Distribution

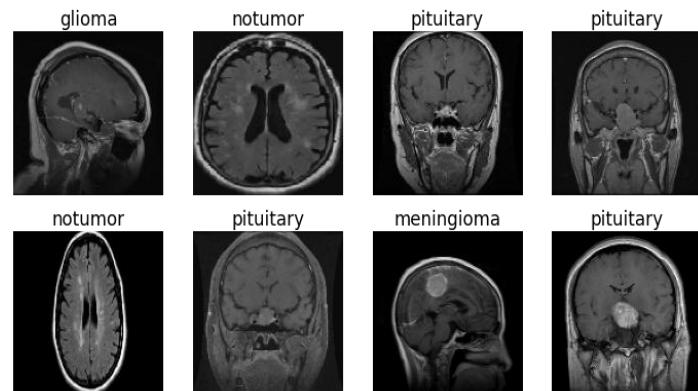


Fig.2. Sample Images

#### 3.2 PRE-PROCESSING

Our proposed system initiates with an image pre-processing application. Typically, MRI images are of high quality, featuring good contrast. To enhance the images further, we apply Gaussian filters to eliminate any potential noise present in the MR images. This filter, often referred to as a smoothing operator, introduces a degree of blur to the images, effectively reducing noise. While this process eliminates subtle visual features that might be inherently present, it is particularly adept at addressing Gaussian noise. The Gaussian function (GF) used in this context to describe the probability distribution of the noise serves as the impulse response for the filter. It is efficient in eliminating Gaussian noise. The GF of this linear low-pass filter acts as a low-pass filter with a specific standard deviation. The convolution process operates on each pixel  $G(i,j)$  in the image, and here’s how it works:

- Place the center of the Gaussian kernel at pixel  $G(i,j)$ .

- Multiply each kernel element with the image’s corresponding pixel value.
- Sum up the results of these multiplications.
- Set the pixel  $G(i,j)$  in the output image to this sum.

Every pixel in the input image goes through this process again, producing an output image that is blurry or smoothed. The convolution operation effectively applies the Gaussian distribution to each pixel, smoothing the image while preserving important features. The present work uses a 2-D Gaussian smoothing kernel of size  $3 \times 3$  and sigma which specifies the standard deviation equals to one. A  $3 \times 3$  Gaussian Kernel (two-dimensional) with Standard Deviation = 1, appears as shown in Fig.3.

|                |   |   |   |
|----------------|---|---|---|
|                | 1 | 2 | 1 |
| $\frac{1}{16}$ | 2 | 4 | 2 |
|                | 1 | 2 | 1 |

Fig.3. A  $3 \times 3$  Gaussian Kernel with  $\sigma = 1$

### 3.3 SEGMENTATION

The brain area in an MRI image was segmented using the snake segmentation approach. The raster scan served as the model for the Snake segmentation process which will cover the boundaries of the image. The objective of this application is to accurately delineate the boundaries for regions of interest within MRI scans. Snake-based segmentation offers deformable contours that can adapt their shapes to get object outline contours. SAC (Snake Active Contour) algorithm [6- 8] is employed for modelling a primary contour in the image space and an energy function (EF) is put forward to characterize the shape of the area by the internal as well as external energy.

The features of curve help to determine the internal energy and the attributes of image assist in describing the external energy including curvature, curve length, etc. EF is diminished to converge the primary contour curve  $C(s)=(x(s),y(s), s \in [0,1])$  continuously to the boundary of the destination region with the restraints of both energies:

$$E(C) = \int_0^1 \alpha E_{int}(C(s)) + E_{img}(C(s) + \gamma E_{con}(C(s))) ds. (1)$$

Three portions are included in EF such as  $E_{int}$  uses to illustrate the internal energy for ensuring that the curve is smooth and regular;  $E_{img}$  is utilized to denote the image energy, assigned by the desired position attributes like edges; the constrained energy is represented with  $E_{con}$ . The SAC algorithm is useful as the geometric restraints are considered. Irrespective of the quality of the image, the major focus is on extracting the closed boundaries. However, some limitations are still there. The challenging task is tackling the region due to its dependence on the first contour. The number, shape and position of control points can acquire the preferred impact only in the case of selecting an appropriate primary contour.

### 3.4 FILTERING

Sometimes, this method can introduce some noise while outlining the boundary of the ROI so the PNLM (Parallel Non-Local Mean) filtering technique was applied to the ROI which further reduced the noise level. The nonlocal means (NLM) filter is the filtering technique which can de-noise the MRI images. It is one of the best image de-noising algorithms because of its superior capability to retain the texture details of an image. The PNLM (Parallel NLM) filter is the improved version of the NLM filter which can de-noise the image more efficiently. A corresponding filter method will be more efficient when it is having the larger value of PSNR. A lower RMSE value indicates better segmentation ability. The results so obtained for a sample image are shown in Table.2.

Table.2. PSNR and MSE Value

|                       | PSNR    | MSE       |
|-----------------------|---------|-----------|
| After Gaussian filter | 11.1149 | 5030.2278 |
| After PNLM filter     | 70.1649 | 0.0063    |

### 3.5 PROPOSED TRANSFER LEARNING BASED DEEP LEARNING MODEL

To predict the tumor type, Transfer learning based Deep learning model is proposed which is the combination of the VGG16 and CNN model. The building block of CNN is a convolutional layer which is mathematically represented as a dot product between two matrices i.e. the original image and the filter matrix. The filter moves over the entire original image to gather information about the various features of the image and thus in this way, a feature map is generated. The VGG16 pre-trained model is used as the transfer learning model over which the CNN model is developed in the presented work.

#### 3.5.1 CNN architecture:

The Fig.4 represents CNN architecture. It is constructed using several layers, such as the input layer, convolution (conv.), pooling, fully connected (FC) layer and output layer.

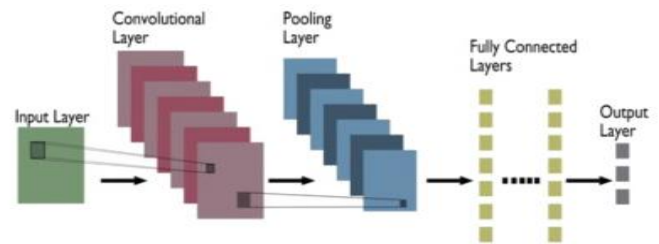


Fig.4. Convolutional Neural Network architecture

#### 3.5.2 VGG16 Model:

The Fig.5 shows the general VGG16 Model architecture. Following are the various details of VGG16 Model:

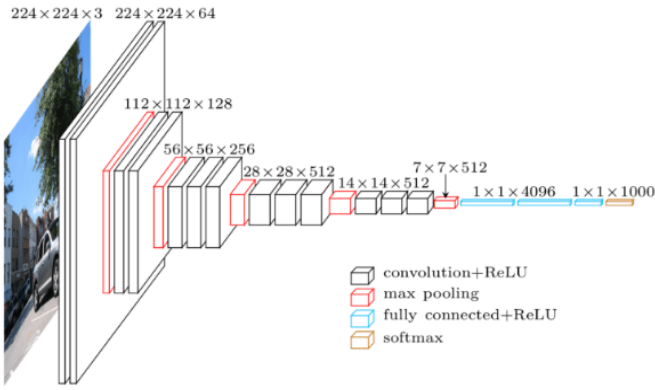


Fig.5. VGG16 Model Architecture

- This model shows sixteen layers, each of which has sixteen weights. There are around 13 convolutional layers, 5 Maxpooling layers and 3 dense layers and these layers contain weights. But there are only 16 weight layers.
- The input of this model is a tensor size of 224 x 224 x 3.
- Because it uses the max pool layer and padding of a 2x2 filter with stride 2, as well as the convolution layers of a 3x3 filter with stride 1, this model uses fewer hyper-parameters than others [116].
- The convolution and max pool layer arrangements are made uniformly across the framework.
- Convolutional layer 1 consist of 64 filters, Convolutional layer-2 comprised of 128 filters, Convolutional layer-3 is having 256 filters, both Convolutional layer-4 and Convolutional layer-5 have 512 number of filters.
- A stack of convolutional layers is present in three fully connected layers: Primary two has 4096 channels, the last of which is used to carry out a 1000-way classification task for the ILSVRC (ImageNet Large Scale Visual Recognition Challenge). As a result, a thousand channels are included. The final layer is referred to as the soft-max layer.

The block diagram of the proposed Transfer learning-based deep learning model is shown in Fig.6. Fig.7 illustrates the architecture of the proposed Transfer Learning-based deep learning model, where the VGG16 model serves as the foundational model following the input layer. At this juncture, the VGG16 model processes input dimensions of 128x128x3 and produces an output of dimensions 4x4x512. Subsequently, the output from the VGG16 model is flattened into a vector. To address overfitting concerns, some randomly selected neurons' output is dropped out from the final output. The activation function employed is ReLu (Rectified Linear Unit), designed to eliminate negative values from the feature map generated after the convolutional layers. This is followed by the application of a Pooling layer, which serves to reduce the dimensionality of the generated feature map. The proposed model incorporates three fully connected layers. The output layer employs the Softmax activation function, confining values to the range between 0 and 1. Ultimately, the output from the transfer learning model manifests as labels corresponding to different tumor categories for which the model has undergone training.

We implemented several other deep learning models and conducted a comparative analysis of their performance with our

proposed model. These included standard CNN, CNN with AlexNet, CNN with a self-attention layer, and CNN with an additive attention layer. In tandem, we applied a similar methodology to implement various machine learning models, including Support Vector Machine (SVM), K Nearest Neighbors (KNN), and Random Forest (RF) classifier, within the same experimental setup. The machine learning (ML) based framework for brain tumor detection is illustrated in Fig.8.

While deep learning models automatically handle the feature extraction step through the neurons of the DL model, machine learning models require human intervention. In the case of machine learning, developers decide the number and types of features for which the model is designed. Specifically, we extracted six GLCM features—Dissimilarity, Correlation, Homogeneity, ASM, Energy, and Contrast—for all four angles (0°, 45°, 90°, and 135°) in our experimental setup.

#### 4. RESULT AND DISCUSSION

This research employs the transfer learning method to identify brain tumors, specifically focusing on the Glioma, Meningioma, Pituitary, and No tumor classes available on the openly accessible Kaggle platform. The dataset used for this study comprises 5712 images, utilized for both training and testing the proposed model. In evaluating the models, key performance metrics such as accuracy, precision, recall, and execution time are considered. These metrics provide insights into the model's effectiveness and efficiency in classifying brain tumors across the specified classes.

##### 4.1 MODELS' PERFORMANCE

The optimal number of epochs for the model is determined through a trial-and-error method, and it is found to be 4. Fig.9 visually presents the training history of all the deep learning models. Two key metrics, namely training accuracy and the loss function, are utilized to evaluate the models' performance during training. The loss function signifies the disparity between the model's predictions and the actual values. In Fig.9 (e), it is demonstrated that during the training of the proposed deep learning model, the loss has decreased from 0.4141 to 0.0744. Simultaneously, the training accuracy has reached 97.36% by the fourth epoch. These graphical representations in Fig.9 effectively illustrate the progress and convergence of the model during the training phase.

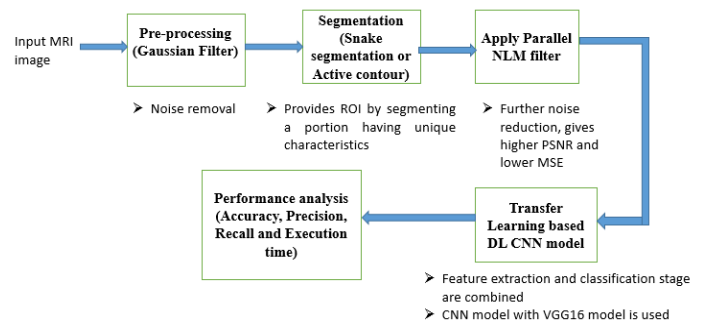


Fig.6. Block diagram of the proposed Transfer learning based deep learning model

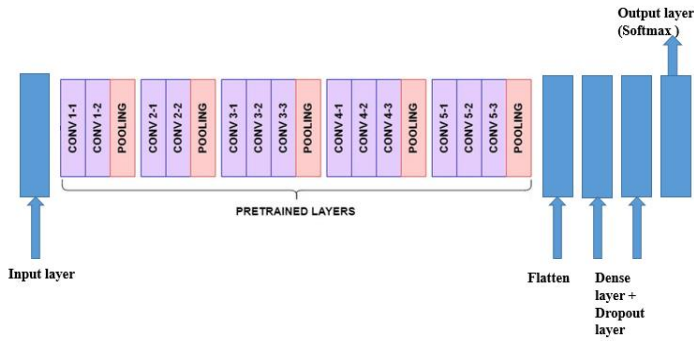


Fig.7. Proposed transfer learning based DL model

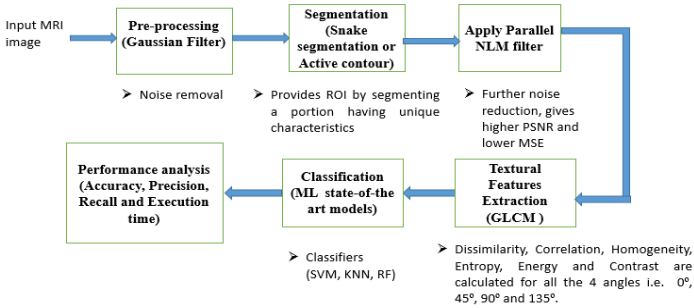
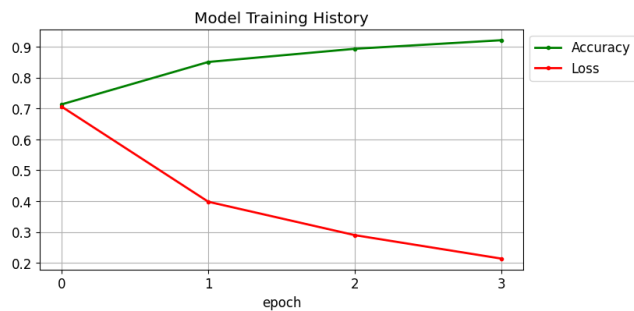


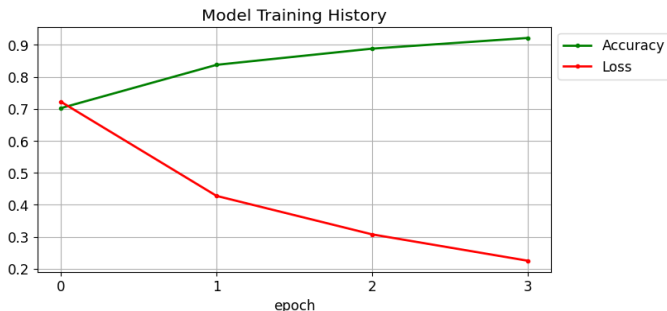
Fig.8. ML Based framework for Brain Tumor Detection



(a) CNN



(b) CNN with Alex Net architecture



(c) CNN with Self-attention layer



(d) CNN with Additive attention layer



(e) Proposed Model

Fig.9. History of training for the various Deep learning model

## 4.2 CONFUSION MATRIX

It is among the simplest and easiest techniques for determining the model's accuracy and correctness. It is applied to classification problems in which there may be two or more different class types in the output. It is a 2D array with dimensions of (K x K) where K denotes the number of classes present in the database. A general confusion matrix for two classes is shown in Fig.10, where, TP = True Positive = Part of a positive class that is correctly predicted TN = True Negative = Part of the Negative class that is correctly predicted FP = False Positive = Part of a positive class that is incorrectly predicted FN = False Negative = Part of a negative class that incorrectly predicted

The confusion matrices for all the machine learning models (SVM, KNN, RF), other implemented Deep learning models and the proposed model are shown in Fig.11. Here, rows of the confusion matrix represent the actual label and columns show the predicted label of the test dataset.

|                  |              | Actual Values |              |
|------------------|--------------|---------------|--------------|
|                  |              | Positive (1)  | Negative (0) |
| Predicted Values | Positive (1) | TP            | FP           |
|                  | Negative (0) | FN            | TN           |

Fig.10 A general 2x2 Confusion matrix

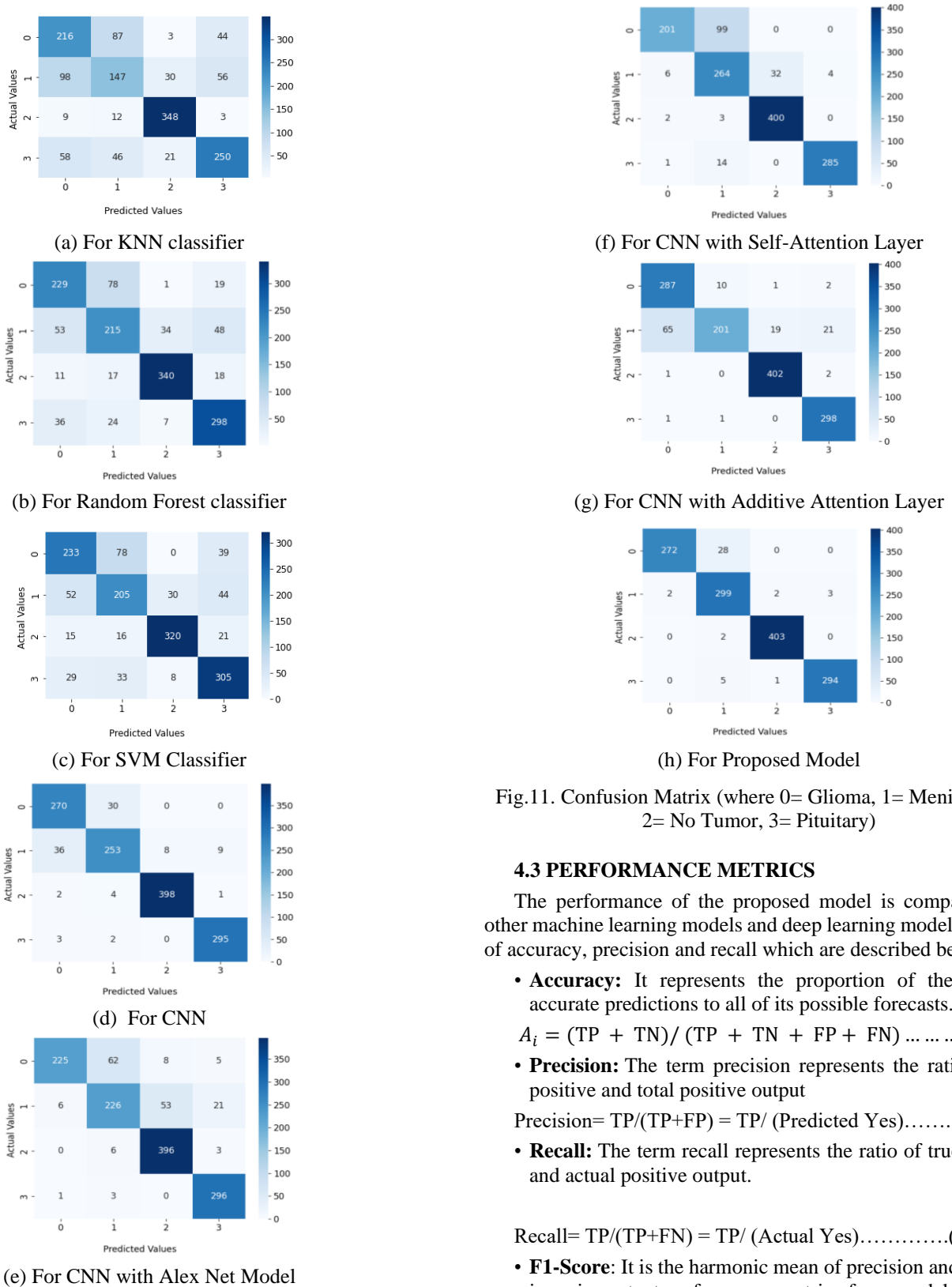


Fig.11. Confusion Matrix (where 0= Glioma, 1= Meningioma, 2= No Tumor, 3= Pituitary)

4.3 PERFORMANCE METRICS

The performance of the proposed model is compared with other machine learning models and deep learning models in terms of accuracy, precision and recall which are described below:-

- **Accuracy:** It represents the proportion of the model’s accurate predictions to all of its possible forecasts.

$$A_i = (TP + TN) / (TP + TN + FP + FN) \dots \dots \dots (7)$$

- **Precision:** The term precision represents the ratio of true positive and total positive output

$$\text{Precision} = TP / (TP + FP) = TP / (\text{Predicted Yes}) \dots \dots \dots (8)$$

- **Recall:** The term recall represents the ratio of true positive and actual positive output.

$$\text{Recall} = TP / (TP + FN) = TP / (\text{Actual Yes}) \dots \dots \dots (9)$$

- **F1-Score:** It is the harmonic mean of precision and recall. It is an important performance metrics for a model when the precision and recall value are approximately the same. Precision, Recall and F1- Score value class label-wise are shown in Table.3.

Table.3. Precision, Recall and F1- score value different class labels of dataset

| A. KNN       |           |        |           | E. CNN with Alex Net |           |        |           |
|--------------|-----------|--------|-----------|----------------------|-----------|--------|-----------|
| Class Labels | Precision | Recall | F1- Score | Class Labels         | Precision | Recall | F1- Score |
| Glioma       | 0.57      | 0.62   | 0.59      | Glioma               | 0.97      | 0.75   | 0.85      |
| Meningioma   | 0.50      | 0.44   | 0.49      | Meningioma           | 0.76      | 0.74   | 0.75      |
| No- Tumor    | 0.87      | 0.94   | 0.90      | No- Tumor            | 0.87      | 0.98   | 0.92      |
| Pituitary    | 0.71      | 0.67   | 0.69      | Pituitary            | 0.91      | 0.99   | 0.95      |

| B. Random Forest |           |        |           | F. CNN with Self Attention Layer |           |        |           |
|------------------|-----------|--------|-----------|----------------------------------|-----------|--------|-----------|
| Class Labels     | Precision | Recall | F1- Score | Class Labels                     | Precision | Recall | F1- Score |
| Glioma           | 0.70      | 0.70   | 0.70      | Glioma                           | 0.96      | 0.67   | 0.79      |
| Meningioma       | 0.64      | 0.61   | 0.63      | Meningioma                       | 0.69      | 0.86   | 0.77      |
| No- Tumor        | 0.89      | 0.88   | 0.89      | No- Tumor                        | 0.93      | 0.99   | 0.96      |
| Pituitary        | 0.78      | 0.82   | 0.80      | Pituitary                        | 0.99      | 0.95   | 0.97      |

| C. SVM       |           |        |           | G. CNN with Additive Attention Layer |           |        |           |
|--------------|-----------|--------|-----------|--------------------------------------|-----------|--------|-----------|
| Class Labels | Precision | Recall | F1- Score | Class Labels                         | Precision | Recall | F1- Score |
| Glioma       | 0.71      | 0.67   | 0.69      | Glioma                               | 0.81      | 0.96   | 0.88      |
| Meningioma   | 0.62      | 0.62   | 0.62      | Meningioma                           | 0.95      | 0.66   | 0.78      |
| No- Tumor    | 0.89      | 0.86   | 0.88      | No- Tumor                            | 0.95      | 0.99   | 0.97      |
| Pituitary    | 0.75      | 0.81   | 0.78      | Pituitary                            | 0.92      | 0.99   | 0.96      |

| D. CNN       |           |        |           | H. Proposed Model |           |        |           |
|--------------|-----------|--------|-----------|-------------------|-----------|--------|-----------|
| Class Labels | Precision | Recall | F1- Score | Class Labels      | Precision | Recall | F1- Score |
| Glioma       | 0.87      | 0.90   | 0.88      | Glioma            | 0.99      | 0.91   | 0.95      |
| Meningioma   | 0.88      | 0.83   | 0.85      | Meningioma        | 0.90      | 0.98   | 0.93      |
| No- Tumor    | 0.98      | 0.98   | 0.98      | No- Tumor         | 0.99      | 1.00   | 0.91      |
| Pituitary    | 0.97      | 0.98   | 0.98      | Pituitary         | 0.99      | 0.98   | 0.98      |

The Table.4 provides the accuracy, precision, recall and execution time metrics value at a glance for different classifiers. Fig.12 depicts that the results of the introduced approach are compared with the ML models (KNN, Random Forest and SVM) and other implemented DL models. The proposed model achieves a training accuracy of 97.36 % and a testing accuracy of 96.7 %. When compared with other machine learning models and other deep learning models such as the KNN Model, Random Forest Model, SVM Model, CNN model, CNN with Alexnet model, CNN with self-attention layer and CNN with additive attention layer which have achieved an accuracy of 67 %, 75.7%, 74.4 %, 92.75, 87.18%, 87.71% and 90.61% respectively for brain tumor detection proves the efficiency and reliability of the proposed model. The code's execution time is determined during its runtime, encompassing the duration from the feature extraction stage to the classification. In the context of the proposed Deep Learning model, the training process for localizing and classifying brain tumors from the MR images dataset extended to 2 hours and 40 minutes. In contrast, the average training time for all machine learning models was approximately 1 hour and 15 minutes. Notably, the deep learning models exhibited an extended training phase, primarily attributed to the increased number of parameters involved.

Table.4. Result Comparison

| Model                             | Accuracy | Precision | Recall | Execution time |
|-----------------------------------|----------|-----------|--------|----------------|
| KNN                               | 67 %     | 66 %      | 67 %   | 1 hr 02 mins   |
| Random Forest                     | 75.7 %   | 75.2 %    | 75.2 % | 1 hr 15 mins   |
| SVM                               | 74.4 %   | 74 %      | 74 %   | 1 hr 07 mins   |
| CNN                               | 92.75 %  | 92 %      | 92%    | 2 hr 44 mins   |
| CNN with Alex Net                 | 87.18 %  | 88 %      | 86 %   | 3 hr 17 mins   |
| CNN with self-attention layer     | 87.71 %  | 89%       | 87 %   | 2 hr 52 mins   |
| CNN with additive attention layer | 90.61 %  | 91 %      | 90 %   | 2 hr 57 mins   |
| Proposed Model                    | 96.7%    | 96 %      | 95 %   | 2 hr 15 mins   |



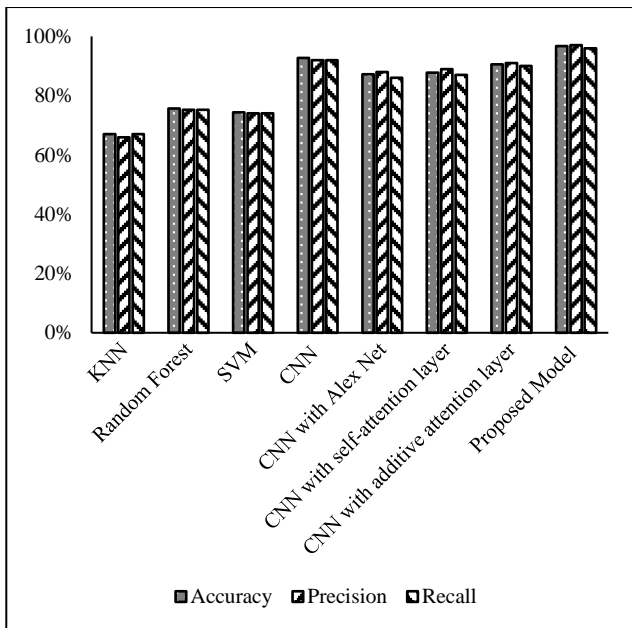


Fig.12. Result Analysis of Different Model

## 5. FUTURE SCOPE OF THE WORK

While the current study utilizes a Kaggle dataset, future work will incorporate multiple datasets from diverse sources to enhance the model's generalizability across various imaging settings and patient demographics. Additionally, the absence of real-world clinical validation is a limitation that will be addressed in future research. This will involve testing the model in clinical environments, potentially through collaborations with healthcare providers, to ensure its effectiveness and reliability in practical medical applications. Optimization techniques can be applied to the pre-processing steps to reduce computational overhead, particularly in resource-limited environments. In the future, fine-tuning strategies will be explored to improve the model's adaptability to novel datasets.

## REFERENCES

- [1] P. Harish and S. Baskar, "MRI Based Detection and Classification of Brain Tumor using Enhanced Faster R-CNN and Alex Net Model", *Materials Today*, Vol. 40, pp. 102-110, 2020.
- [2] G. Manogaran, P.M. Shakeel, A.S. Hassanein, P. Malarvizhi Kumar and G. Chandra Babu, "Machine Learning Approach-Based Gamma Distribution for Brain Tumor Detection and Data Sample Imbalance Analysis", *IEEE Access*, Vol. 7, pp. 12-19, 2019.
- [3] R. Hashemzahi, S.J.S. Mahdavi and S.R. Kamel, "Detection of Brain Tumors from MRI Images Base on Deep Learning using Hybrid Model CNN and NADE", *Biocybernetics and Biomedical Engineering*, Vol. 2, pp. 3154-3162, 2020.
- [4] G. Deepa, G. Leena Rosalind Mary and M. Dharanisri, "Detection of Brain Tumor using Modified Particle Swarm Optimization Segmentation via Haralick Features Extraction and Subsequent Classification by KNN Algorithm", *Materials Today*, Vol. 41, pp. 114-121, 2021.
- [5] S. Kumar, C. Dabas and S. Godara, "Classification of Brain MRI Tumor Images: A Hybrid Approach", *Procedia Computer Science*, Vol. 122, pp. 510-517, 2017.
- [6] M. Li, L. Kuang, S. Xu and Z. Sha, "Brain Tumor Detection based on Multimodal Information Fusion and Convolutional Neural Network", *IEEE Access*, Vol. 7, pp. 180134-180146, 2019.
- [7] A. Hossain, "A YOLOv3 Deep Neural Network Model to Detect Brain Tumor in Portable Electromagnetic Imaging System", *IEEE Access*, Vol. 9, pp. 82647-82660, 2021.
- [8] D. Rammurthy and P.K. Mahesh, "Whale Harris Hawks Optimization based Deep Learning Classifier for Brain Tumor Detection using MRI Images", *Journal of King Saud University - Computer and Information Sciences*, Vol. 51, No. 12, pp. 5859-5870, 2020.
- [9] N. Kesav and M.G. Jibukumar, "Efficient and Low Complex Architecture for Detection and Classification of Brain Tumor using RCNN with Two Channel CNN", *Journal of King Saud University - Computer and Information Sciences*, Vol. 31, No. 5, pp. 1747-1756, 2021.
- [10] Md. S.I. Khan, A. Rahman and I. Dehzangi, "Accurate Brain Tumor Detection using Deep Convolutional Neural Network", *Computational and Structural Biotechnology Journal*, Vol. 20, No. 1, pp. 4733-4745, 2022.
- [11] A. Han, "Combining Noise-to-Image and Image-to-Image GANs: Brain MR Image Augmentation for Tumor Detection," *IEEE*, Vol. 7, pp. 156966-156977, 2019.
- [12] E. Dandil and S. Karaca, "Detection of Pseudo Brain Tumors via Stacked LSTM Neural Networks using MR Spectroscopy Signals", *Biocybernetics and Biomedical Engineering*, Vol. 41, No. 5, pp. 173-195, 2020.
- [13] F. Ozyurt, E. Sert and D. Avci, "An Expert System for Brain Tumor Detection: Fuzzy C-means with Super Resolution and Convolutional Neural Network with Extreme Learning Machine", *Medical Hypotheses*, Vol. 22, No. 6, pp. 1754-1764, 2019.
- [14] M. Sharif, J. Amin and S. Chandra Satapathy, "An Integrated Design of Particle Swarm Optimization (PSO) with Fusion of Features for Detection of Brain Tumor", *Pattern Recognition Letters*, Vol. 129, pp. 150-157, 2019.
- [15] H. Abdel-Gawad, L.A. Said and A.G. Radwan, "Optimized Edge Detection Technique for Brain Tumor Detection in MR Images", *IEEE Access*, Vol. 8, pp. 136243-136259, 2020.
- [16] P.S. Kumar, S.B. Shaik and H. Mulam, "High-Performance Compression-Based Brain Tumor Detection using Lightweight Optimal Deep Neural Network", *Advances in Engineering Software*, Vol. 10, No. 11, pp. 2464-2468, 2022.
- [17] M. Thachayani and S. Kurian, "AI Based Classification Framework for Cancer Detection using Brain MRI Images", *Proceedings of International Conference on System, Computation, Automation and Networking*, pp. 1-4, 2021.
- [18] M.K. Islam, M.S. Ali and M.A. Hossain, "Brain Tumor Detection in MR Image using Superpixels, Principal Component Analysis and Template based K-means Clustering Algorithm", *Machine Learning with Applications*, Vol. 4, No. 3, pp. 717-730, 2021.
- [19] A.S. Derea, H.K. Abbas, H.J. Mohamad and A.A. Al-Zuky, "Adopting Run Length Features to Detect and Recognize

- Brain Tumor in Magnetic Resonance Images”, *Proceedings of International Conference on Computer and Applied Sciences*, pp. 186-192, 2019.
- [20] K. Saruladha, “Design of FCSE-GAN for Dissection of Brain Tumor in MRI”, *Proceedings of International Conference on Smart Technologies in Computing, Electrical and Electronics*, pp. 1-6, 2020.
- [21] A.S. Reddy, “Effective CNN-MSO Method for Brain Tumor Detection and Segmentation”, *Materials Today: Proceedings*, Vol. 8, No. 2, pp. 766-777, 2021.
- [22] M. Jian, X. Zhang and H. Yu, “Tumor Detection in MRI Brain Images Based on Saliency Computational Modeling”, *IFAC-Papers OnLine*, Vol. 1, No. 9, pp. 611-619, 2020.
- [23] H.A. Shah, F. Saeed, S. Yun, J.H. Park, A. Paul and J.M. Kang, “A Robust Approach for Brain Tumor Detection in Magnetic Resonance Images using Finetuned Efficient Net”, *IEEE Access*, Vol. 10, pp. 65426-65438, 2022.
- [24] M.A. Kabir, “Early-Stage Brain Tumor Detection on MRI Image using a Hybrid Technique”, *Proceedings of IEEE Region 10 Symposium on Image and Video Processing*, pp. 1828-1831, 2020.